RSC Advances

PAPER

View Article Online
View Journal | View Issue

Cite this: *RSC Adv.*, 2024, **14**, 38416

Augmented triboelectric properties of graphene-filled poly(vinylidene difluoride-*co*-hexafluoropropylene) (PVDF-HFP) nanofibers

Chen-Hung Lee,[a] Wei-Kang Huang,[b] Meng-Fang Lin, *[c] Yi-Hua Kuo,[b] Shih-Jung Liu *[bd] and Hiroshi Ito [e]

Triboelectric nanogenerators (TENGs) are devices that convert mechanical energy into electrical energy through the triboelectric effect, supplying power to a wide array of advanced sensing and monitoring systems. In this work, we utilized graphene-filled nanofibrous poly(vinylidene difluoride-*co*-hexafluoropropylene) (PVDF-HFP) as TENGs, employing electrospinning technology. We examined how the dielectric characteristics and transferred charge of the electrification mat affect the output of TENGs. By including graphene nanofillers, the 15 wt% graphene/PVDF-HFP electrospun nanofiber TENG achieved a peak output voltage of 1024 V and a relevant current density of 1.11 μA cm^{-2}. The improved performance of the electrospun graphene/PVDF-HFP nanofibrous TENGs could be attributed to increased interface polarization and enhanced charge transfer, indicating more effective seize and storage of triboelectric electrons. Furthermore, the fabricated TENGs remained stable when tested for over 20 000 cycles and were capable of powering an array of 1000 light-emitting diode bulbs. The electrospun graphene-filled nanofibrous TENGs demonstrated significant potential for collecting mechanical energy and supplying power to electronic devices.

Received 22nd October 2024
Accepted 27th November 2024

DOI: 10.1039/d4ra07550a

rsc.li/rsc-advances

1. Introduction

Triboelectric nanogenerators (TENGs) are cutting-edge devices that transform mechanical energy into electrical energy using the triboelectric effect, where materials acquire an electric charge through contact and subsequent separation. By utilizing this effect, TENGs consist of layers of different materials that generate a voltage when subjected to friction or pressure changes, due to the transfer of electrons. This technology harnesses everyday mechanical movements, such as walking or vibrations, and transforms them into useable electrical power. The versatility and efficiency of TENGs make them ideal for a range of applications, including powering wearable electronics, harvesting energy from environmental sources, and enabling self-powered sensors. These attributes highlight their potential to revolutionize energy harvesting and portable power solutions.[1,2]

The working principle of a TENG relies on the interplay between contact electrification and electrostatic induction. In this process, contact electrification generates static polarized charges, while electrostatic induction serves as the primary mechanism that alters mechanical energy into electrical energy.[3–5] TENGs typically resemble a variable-gap plate capacitor, leading to capacitive behavior such as increased charge storage, which boosts their performance.[6–11] Consequently, the efficiency of a TENG is influenced by the dielectric constant of the triboelectric layer. While poly(vinylidene difluoride-*co*-hexafluoropropylene) (PVDF-HFP)[12,13] has been the most widely used material for preparing TENGs, the raw polymers typically employed in TENGs often yield comparatively low triboelectric outputs, which are inadequate for feasible use.

Graphene, a single layer of carbon atoms arranged in a two-dimensional honeycomb lattice, possesses remarkable electrical properties due to its unique structure.[14] This nanomaterial offers significant advantages for TENG applications. Graphene is both incredibly strong and flexible, allowing TENGs to withstand mechanical stress and deformation, which enhances their durability and performance, particularly in flexible and wearable applications.[15] Its high surface area provides more contact area for the triboelectric effect, which can increase the amount of generated electrical energy. The high electron mobility of graphene facilitates rapid charge separation and transfer, critical for the efficient operation of TENGs. Graphene is chemically stable and resistant to

[a]*Division of Cardiology, Department of Internal Medicine, Chang Gung Memorial Hospital-Linkou, Chang Gung University College of Medicine, 33302 Taoyuan, Taiwan*
[b]*Department of Mechanical Engineering, Chang Gung University, 259, Wen-Hwa 1st Road, Kwei-Shan, Taoyuan 33302, Taiwan. E-mail: shihjung@mail.cgu.edu.tw*
[c]*Department of Materials Engineering, Ming Chi University of Technology, New Taipei City, Taiwan. E-mail: mflin@mail.mcut.edu.tw*
[d]*Department of Orthopedic Surgery, Bone and Joint Research Center, Chang Gung Memorial Hospital at Linkou, Taoyuan 33305, Taiwan*
[e]*Graduate School of Organic Materials Science, Yamagata University, Yonezawa, Yamagata 992-8510, Japan*

environmental degradation, ensuring the durability and reliability over time of TENGs in distinct conditions. Additionally, the lightweight nature of graphene contributes to the development of portable and wearable TENGs without adding significant bulk. The mechanical and electrical of graphene can also be adjusted through various methods, including chemical doping and functionalization, allowing for optimization according to specific TENG applications. Its transparency allows for the development of transparent TENGs, which can be integrated into display technologies and windows for energy harvesting without obstructing visibility.[16]

The performance of TENGs is primarily influenced by the choice of a positive and negative triboelectric surface pair (tribosurfaces).[17,18] Enhancing surface roughness generally improves TENG output by enhancing the effective contact area, which boosts the induction of triboelectric charges.[19–21] This enhancement can be achieved using various rough tribosurfaces, such as films with inherent microscale roughness,[22] microscale-replicated bumpy surfaces,[23] narrow grated surfaces,[24] sub-micrometer-scale etched surfaces,[20] and elestrospun nanofibers.[25,26] Electrospinning is an efficient process for producing nanofibrous membranes from various polymers.[27] It includes using a high-voltage electric field to a polymer solution or melt, which is then ejected through a small nozzle. As the charged polymer jet is stretched and thinned, it solidifies into continuous fibers with diameters ranging from nanometers to micrometers. This process allows precise control over the fiber diameter, porosity, and overall architecture of the resulting membranes. The electrospun nanofibers exhibit high surface area-to-volume ratios, excellent flexibility, and customizable thickness.[28] The inherent high surface roughness and micro/nano-scale architecture of electrospun membranes enhance their performance in TENGs, improving contact area and friction effects to maximize energy output. Compared to other methods of introducing micro/nanostructures into electro-frictional layers to enhance surface charge density and, consequently, the performance of the triboelectric harvester, the electrospinning setup is relatively simple and cost-effective. This simplicity also translates to lower operational costs and easier maintenance.

In this work, we utilized graphene-filled nanofibrous PVDF-HFP mats as TENGs through the electrospinning process. While previous studies have developed graphene-filled PVDF nanofibers,[29] PVDF-HFP offers several advantages over PVDF for triboelectric nanogenerators (TENGs). Its copolymer structure, which includes hexafluoropropylene (HFP), provides enhanced flexibility and mechanical resilience,[30] making PVDF-HFP more suitable for flexible and wearable TENG applications. This flexibility also improves durability under repeated deformation. Additionally, PVDF-HFP has a higher dielectric constant, which enhances charge storage capability and thus boosts energy conversion efficiency. The copolymer structure promotes the formation of the electroactive β-phase, recognized for its high dipole moment, which increases surface charge density and enhances overall triboelectric performance. PVDF-HFP also demonstrates improved miscibility with fillers, enabling further enhancement of dielectric properties and charge density when combined with nanoparticles. Furthermore, it is easier to process, facilitating porous structure formation for greater surface area, and it has improved environmental stability, which ensures long-term reliability. To the best of the authors' knowledge, no research to date has investigated the use of graphene/PVDF-HFP composite nanofibers for TENGs. After fabrication, we examined how the altered dielectric characteristics and transferred charge of the electrification film affected TENG output. The stability of the TENGs was also evaluated, and the developed TENGs' capability to power an LED array was demonstrated.

2. Materials and methods

2.1 Materials

The nanofiber material, PVDF-HFP with a molecular weight (Mw) of 455 kDa, was sourced from Sigma-Aldrich, MO, USA. The solvent, dimethylformamide (DMF), and graphene nanopowder (8 nm flakes) were also acquired from Sigma-Aldrich.

2.2 Preparation of graphene filled nanofibrous mats

Nanofiller-loaded nanofibrous mats with various percentages of graphene, namely 0.5%, 5%, 15% and 25%, were prepared (Table 1). To prepare the 0.5% one, 1.0 g of PVDF-HFP and 5 mg of graphene were blended with 4 mL of DMF. The solution was subsequently magnetically stirred at 60 °C for 24 hours and electrospun employing a lab-built spinning apparatus,[31] with a voltage of 16 kV, a flow rate of 1.0 mL h^{-1}, and a distance of 150 mm between the needle and the collection plate mounted on a reciprocating platform. All electrospinning experiments were conducted at room temperature. The electrospinning of nanofibers with different percentages of graphene followed the same protocol, except that the weights of added graphene varied. For comparison purposes, pristine PVDF-HFP nanofibers were also electrospun. To remove any residual solvent, all spun nanofibers were subjected to vacuum drying at 40 °C for 72 hours.

2.3 Characterization of spun nanofibrous mats

Field emission scanning electron microscopy (FESEM, JEOL JSM-7500F, Tokyo, Japan) was utilized to analyze the morphological structure of the nanofibers post gold coating. The mechanical properties of the nanofibrous graphene/PVDF-HFP membranes were assessed using a Lloyd tensiometer (Ametek,

Table 1 Compositions of graphene filled nanofibrous mats[a]

PVDF-HFP (g)	Graphene (mg)	Graphene (w)/PVDF-HFP (w) (%)
1	0	0
1	5	0.5
1	50	5
1	150	15
1	250	25

[a] DMF used was 4 mL.

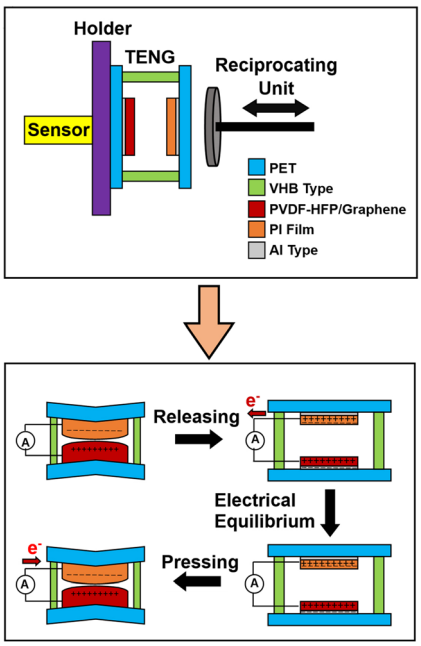

Fig. 1 Schematically the working mechanism of lab-made TENGs.

USA) equipped with a 2500 N load cell. The force and elongation at the point of membrane failure were recorded. X-ray diffraction (Malvern Panalytical, Malvern, United Kingdom) was employed to identify the α, β, and γ phase distribution of PVDF-HFP in the electrospun mats. Dielectric constants were determined with an M6632 apparatus (Microtest, Taipei, Taiwan), while charge transfer was assessed using a Keithley 6517B electrometer (Beaverton, OR, USA). In addition, the performance of electrospun graphene/PVDF-HFP mats was conducted on a lab-made TENG. The working mechanism was shown schematically in Fig. 1.[25] A Tektronix DPO 3040 oscilloscope was employed to record the voltage and current outputs from the triboelectric device. Additionally, a magnetic shaker (Sinocera JZK-20) was used to apply dynamic mechanical pressure, with varying forces from 1 to 40 N and frequencies from 1 to 10 Hz. An Arduino UNO R3 with an Atmega 328p microcontroller was employed to construct the LED dimmer switch.

3. Results and discussion

Fig. 2 shows SEM images of electrospun graphene/PVDF-HFP nanofibers with different graphene concentrations. With the addition of graphene, encapsulated beads become visible in the images. Previous study[32] has shown that these additional beads can improve electrical performance by increasing surface roughness. When the graphene content was increased to 25%, irregularly shaped beads and a rough distribution of nanofibers were observed. The tensile properties of the graphene/PVDF-HFP nanofiber mats were measured and are shown in Fig. 3. The electrospun nanofibrous mats demonstrate good flexibility and extensibility, with 20% elongation before breaking.

Fig. 4 presents the XRD patterns of graphene-filled PVDF-HFP nanofibrous mats produced with different weight percentages. The XRD profiles of the pure PVDF-HFP nanofibrous mats exhibit distinct peaks corresponding to the α, β, and γ crystal phases of PVDF. Specifically, the peak at 17.9° is associated with the PVDF α-phase, while the broad vibration at 19.2° represents the overlapping diffraction of the β-phase. A characteristic peak of graphene is observed at 26.5°. With the increase of graphene amount in nanofibers, the intensity of the graphene peaks increases compared to those of the pure PVDF-HFP.

The electrical properties of the graphene/PVDF-HFP mats were investigated. Fig. 5 illustrates how different weight percentages of graphene affect the dielectric constant of nanofibrous mats under various frequencies of an externally imposed electric field. Additionally, the polarizability of a dielectric material depends on the frequency of the imposed electric field, which in turn impacts its capacitance and relative permittivity. Dipoles in a dielectric material align with an

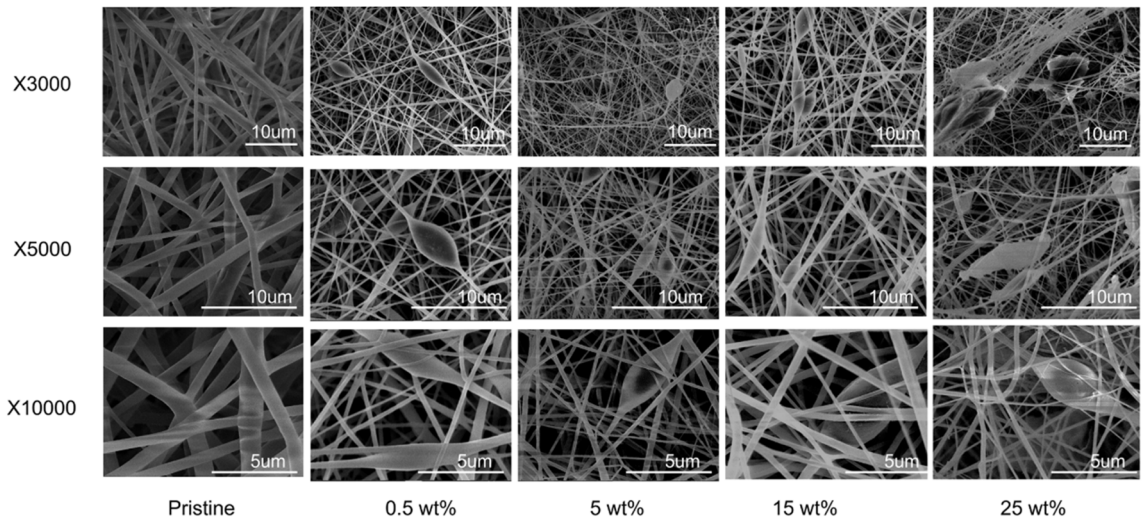

Fig. 2 Microimages of electrospun nanofibers with different contents of graphene.

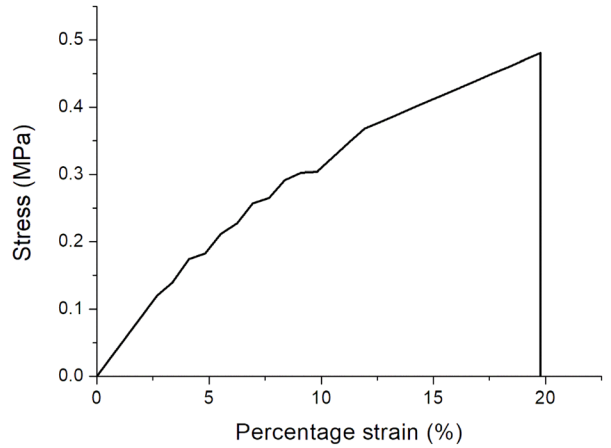

Fig. 3 Stress–strain curve of the 15% graphene-filled PVDF-HFP nanofibers.

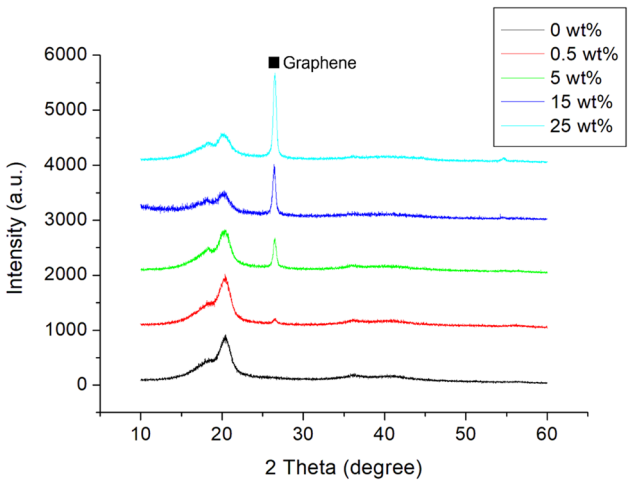

Fig. 4 XRD patterns of the PVDF-HFP nanofibers filled with different percentages of graphene.

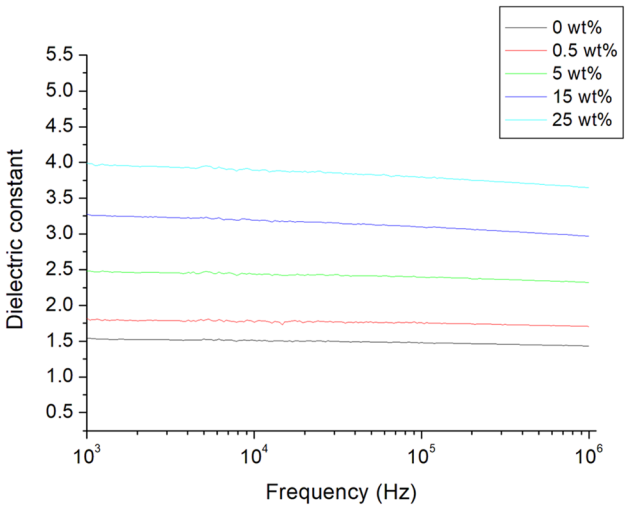

Fig. 5 Frequency-dependence of the dielectric constant of graphene/PVDF-HFP nanofibrous mats.

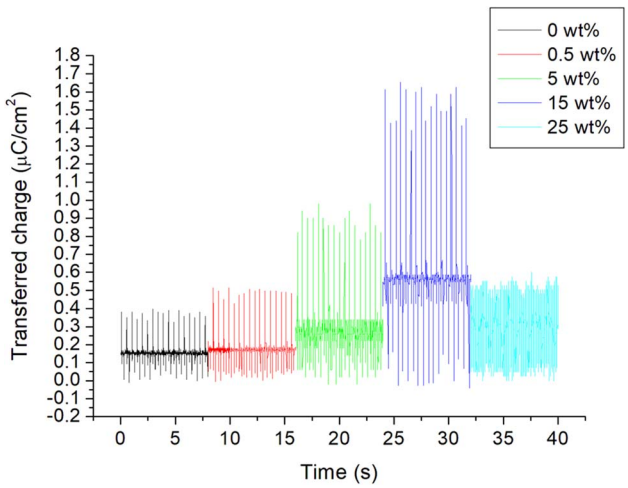

Fig. 6 Transferred charge of different percentage graphene/PVDF-HFP nanofibrous mats.

external electric field, contributing to the material's polarization. At lower frequencies, the field alternates slowly, giving dipoles sufficient time to reorient and align with each change in field direction, resulting in higher dielectric permittivity. However, as frequency increases, the time available for dipoles to realign with the rapidly changing field decreases. Eventually, at high enough frequencies, dipoles can no longer keep pace with the field's oscillations, leading to a decrease in permittivity.[33,34]

Based on the correlation between dynamic capacitance and transferred charge in TENGs, an increase in interfacial polarization enhances TENG performance. Furthermore, the dielectric constants increased with the addition of graphene nanofillers, attributed to interfacial polarization, which boosts TENG output. However, the dielectric constants of all spun nanofibrous mats remained comparatively low due to their highly porous structures, which contain air—a substance with a low dielectric constant—thereby reducing the overall dielectric properties.

Fig. 6 shows that the transferred charge increased with the graphene content up to 15 wt%, after which it decreased, likely owing to higher dielectric loss as the nanofiller content was increased to 25 wt%. The 15 wt% graphene/PVDF-HFP nanofibrous mats exhibited the highest transferred charge because of their elevated dielectric value and reduced dielectric loss. The rise in transferred charge was due to enhanced seize and management of triboelectric electrons, which subsequently boosted the performance.

The electrical output of spun graphene/PVDF-HFP nanofibers with different weight percentages was measured, and the results are presented in Fig. 7a. The data clearly show that the generated voltage and current arise with the graphene content up to 15%, owing to greater amounts of transferred charge, after

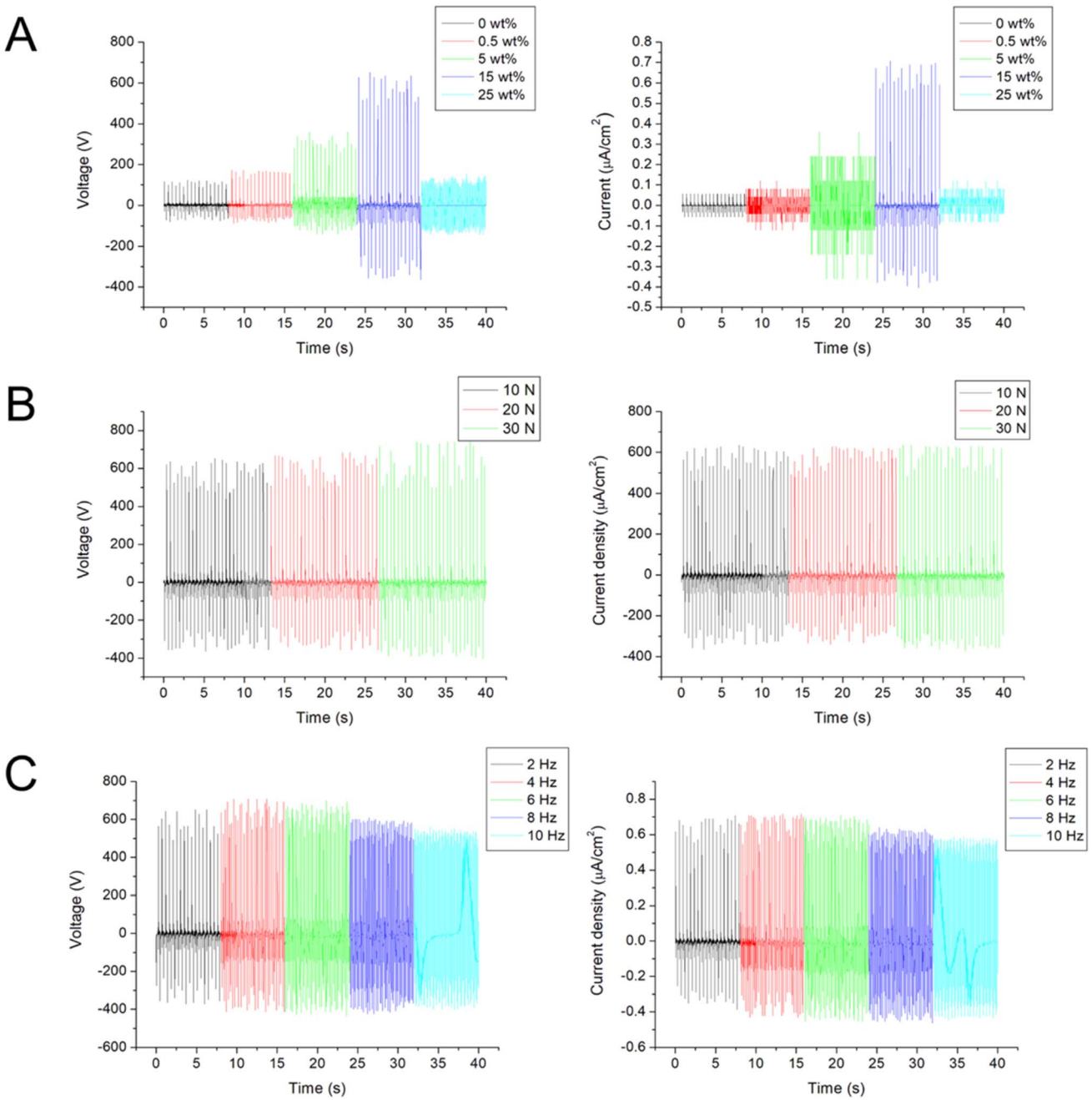

Fig. 7 Maximum output voltage and current density of the nanofibrous TENGs subject to different (A) graphene percentage, (B) applied external force, and (C) operating frequency. (Nanofibrous mats with 15% graphene/PVDF-HFP were used).

which they begin to decline. The 15 wt% graphene/PVDF-HFP electrospun nanofiber TENG achieved a peak voltage of 1024 V, accompanied by a current density of 1.11 μA cm^{-2}. As a nanofiller, graphene's outstanding electrical conductivity facilitates efficient charge transfer, enhancing the overall energy conversion efficiency of TENGs. Consequently, the electrical properties of PVDF-HFP nanofibers improved with the addition of graphene. However, when the graphene content is too high, the structure of the electrospun nanofibers deteriorates, leading to irregular nanofiber distribution, as shown in Fig. 2. This irregular distribution can impede the transfer of electrical charges, ultimately reducing the generated voltage and current of the TENGs.

The influence of the operating frequency and applied external force on the electrical output was investigated. The measured results in Fig. 7b suggest that the electrical output increased slightly with the operating frequency from 2 Hz to 4 Hz, but thereafter, the output decreased as the frequency increased. Meanwhile, the effect of the applied force on the performance was limited (Fig. 7c). Wu *et al.*[26] created ceramic powder-based TENGs featuring electrospun fibrous surfaces made from PVDF-HFP, which included dispersed Eu_2O_3-doped

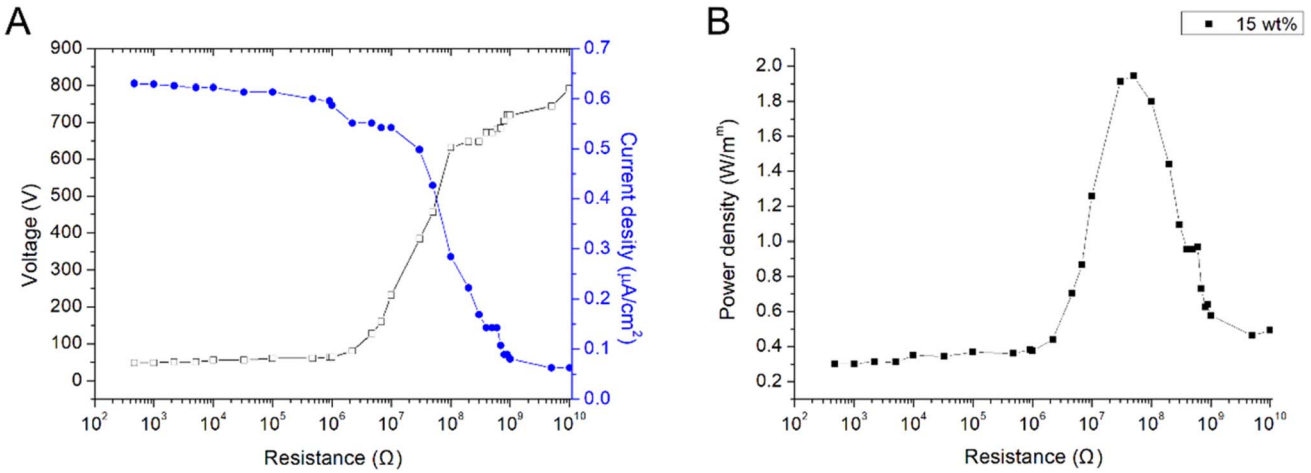

Fig. 8 (A) Output voltage and current density, and (B) power density of TENGs composed of different-weight-percentage graphene filled PVDF-HFP nanofibers.

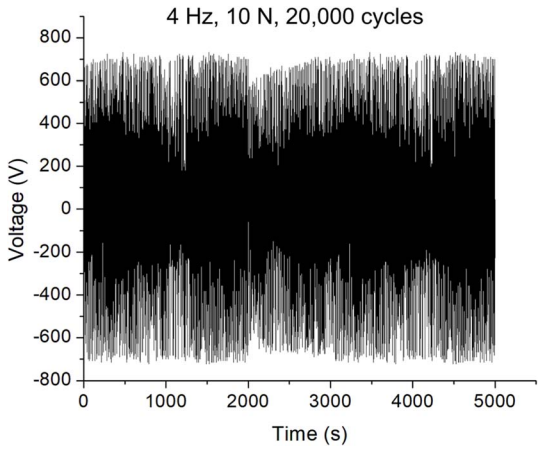

Fig. 9 Long-term cycling test of TENGs (operating conditions: 4 Hz, 10 N, 20 000 cycles).

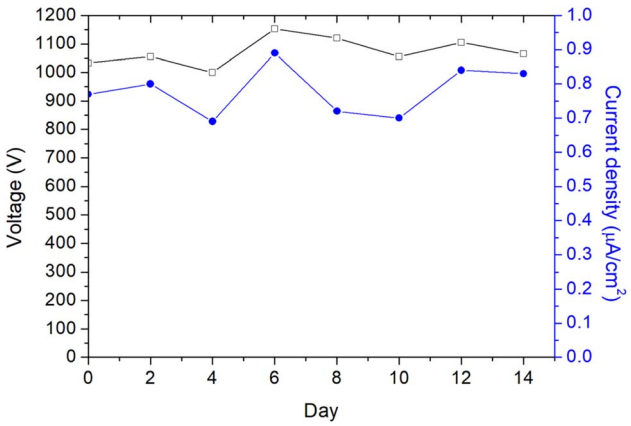

Fig. 10 Stability of output performance of TENGs for 14 days.

$BaTiO_3$ nanofillers. They discovered that enhancing the compressive force or operating frequency led to a substantial increase in electric charges. The experimental outcomes in this study suggested that the influence of applied force or operating frequency is limited. This might be because, compared to ceramic materials, graphene is an excellent conductor of electricity due to its high charge carrier mobility, which can exceed 200 000 $cm^2\ V^{-1}\ s^{-1}$ at room temperature—much higher than that of traditional conductors like copper and silicon. The addition of graphene to PVDF-HFP can thus significantly enhance the electrical properties of the TENGs, enabling high output even with a small force and low operating frequency. Based on these results, for the subsequent experiments, we determined that applying a cyclic compressive force of 10 N at a frequency of 4 Hz provided the optimum operating parameters.

Fig. 8a and b illustrate the electrical characteristics of the 15 wt% graphene/PVDF-HFP nanofibrous TENG under different external load resistances ranging from 470 to 1000 MΩ, when operated at 4 Hz and subjected to a 10 N force. As the load resistance exceeded roughly 10 MΩ, the output voltage rose, while the output current density diminished with the increasing resistance. Based on the theory of impedance matching, the output power reaches its maximum when the external load resistance matches the internal resistance of the power supply (in this case, the TENG's internal resistance). The 15 wt% graphene/PVDF-HFP TENG achieved a peak output power density of 1.95 W m^{-2} at 50 MΩ.

Reliability, durability, and stability are crucial for the practical application of any TENG. To assess the mechanical stability of our device, we monitored the electrical output voltage of the 15 wt% graphene/PVDF-HFP electrospun nanofiber TENG over 20 000 cycles; as shown in Fig. 9, the device demonstrated excellent durability. Fig. 10 shows that the TENG's performance remained consistent even after being stored for 2 weeks.

Finally, the 15 wt% graphene-filled nanofibrous TENGs were also able to power a 1000-LED bulb array, as depicted in Fig. 11. Fig. 12 presents the voltage curves recorded while charging capacitors with various capacitances (0.1, 1, 2.2, 4.7 and 10 μF)

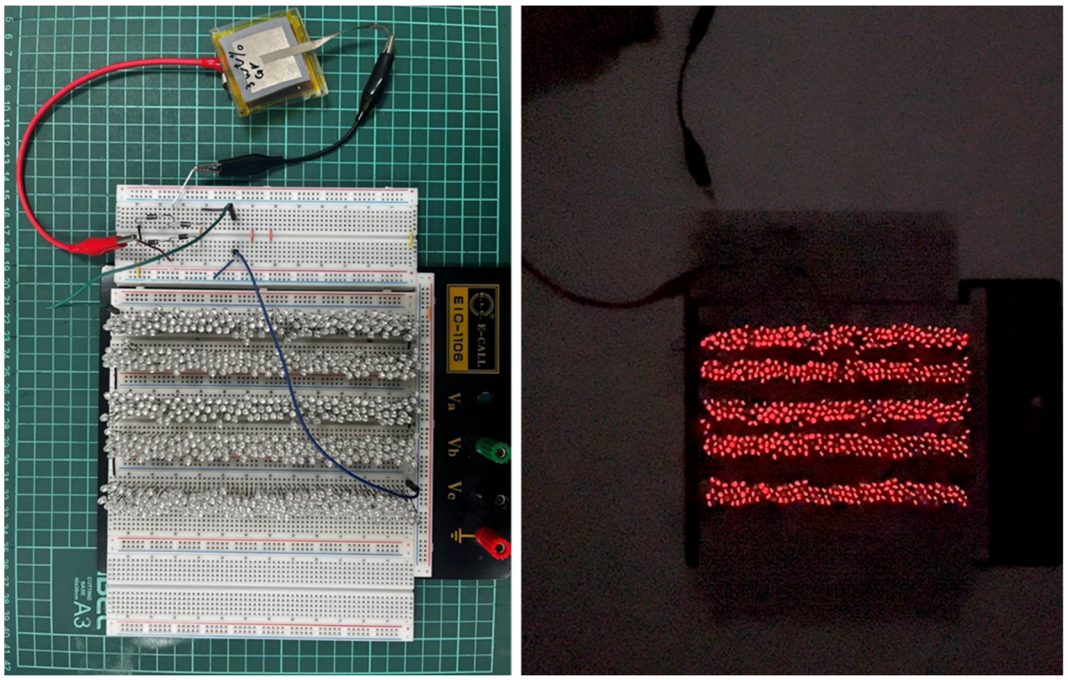

Fig. 11 The 15 wt% graphene-filled nanofibrous TENGs could power a 1000-LED bulb array.

using the graphene/PVDF-HFP TENG. Notably, the 0.1 μF capacitor charged quickly to 25 V in just 38 seconds. The energy stored in these capacitors was 0.031, 0.153, 0.106, 0.135 and 0.076 mJ, respectively, calculated using the formula $E = 1/2 \times$ capacitance $\times$ (voltage)^2.

To date, several studies have been conducted on the development of graphene-based TENGs. Shankaregowda *et al.*[35] developed a flexible, transparent nanogenerator using graphene grown *via* chemical vapor deposition as one of the friction layers. The graphene, deposited on copper, was transferred onto polyethylene terephthalate (PET) using a wet transfer technique, giving the TENG both electrical conductivity and high optical transparency. To enhance its performance, a fluorocarbon plasma-treated thin polydimethylsiloxane (PDMS) layer was fabricated as the second friction layer. The graphene-based TENG achieved a maximum output voltage of 650 V and

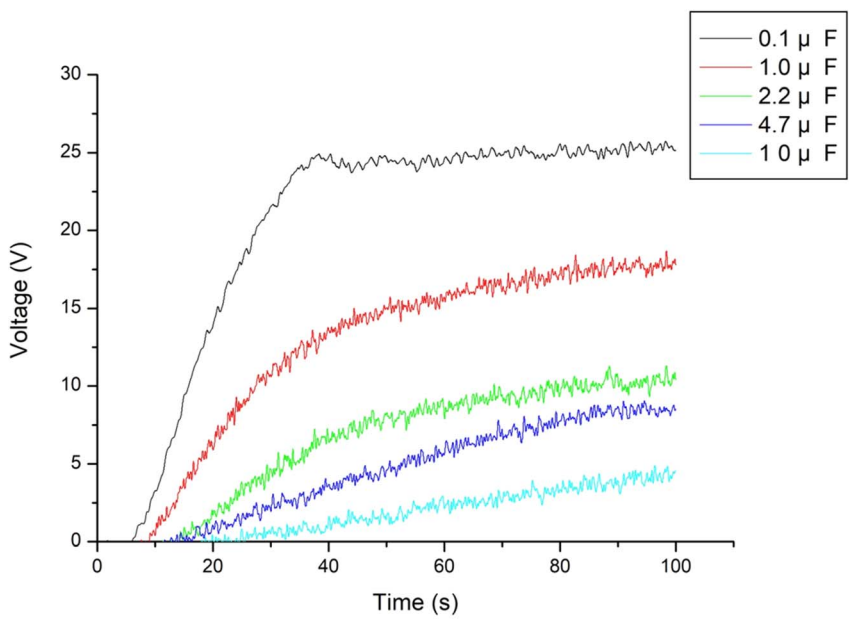

Fig. 12 The voltage curves recorded while charging capacitors with various capacitances (0.1, 1, 2.2, 4.7 and 10 μF) using the graphene/PVDF-HFP TENGs.

a current of 12 μA at a frequency of 4.3 Hz, sufficient to power 50 commercial blue LEDs. Shabbir *et al.*[36] introduced an innovative rolling-type TENG featuring a metal layer and graphene nanoplatelet-doped PDMS. The incorporation of these materials enhanced the TENG's dielectric value and charge custody capacity, resulting in higher electrical output and reduced surface wear. Compared to a pristine device, the modified TENG produced an open-circuit peak voltage of 75.2 V and a short-circuit peak current of 7.36 μA. Furthermore, with a dual-side double-belt configuration, the output increased to 164 V and 10 μA. Pillai *et al.*[37] explored the energy-harvesting capabilities of graphene oxide decorated with silver nanoparticles (GO-AgNPs) in a freestanding nanogenerator setup, utilizing GO-AgNP paper combined with Teflon fabric. Their results demonstrated that the device could produce a peak output power of 40 μW at a voltage of 0.2 V. Jelmy *et al.*[38] proposed a triboelectric nanogenerator (TENG) employing PDMS enhanced with binary hybrids of GO and conducting polymers (CPs) like polyaniline or polypyrrole. These hybrids were incorporated into PDMS through an ultrasonication-assisted dispersion method at room temperature. They found that varying the GO and CP ratios altered the dielectric characteristics of the PDMS composite through different mechanisms including electronic, vibrational, orientation, ionic, and interfacial polarization. Additionally, the electron donor–acceptor interaction between PDMS and the GO/CP fillers increased the surface charge density, thereby improving the overall TENG output. Their tests demonstrated a current of 40 nA and 208 V from finger tapping, and a short-circuit current of 2 mA and 27 V from foot stamping or walking. Sahoo *et al.*[39] engineered a multilayer TENG incorporating graphene, designed using a layer-by-layer assembly approach. To boost charge density, they innovatively introduced an Al_2O_3 charge trapping layer (CTL) between the positive triboelectric layer and the conductive electrode, resulting in a highly flexible TENG. The device demonstrated remarkable durability, maintaining stability after more than 2000 continuous cycles of operation and successfully powering 20 green LEDs. Domingos *et al.*[40] developed TENGs by combining graphene with polymers like PDMS using cost-effective solution processing techniques. The resulting TENG devices exhibited open-circuit voltages around 233 V and short-circuit currents of approximately 731 nA when operated at a frequency of 1.5 Hz. Additionally, a power density of 13.14 μW cm^{-2} was achieved under a load resistance of 200 MΩ. Ejehi *et al.*[41] developed a flexible TENG using GO paper as the electrode. In vertical contact-separation mode, the device achieved a power density of 1.3 W m^{-2}, an open-circuit voltage of up to 870 V, and a current density of 1.4 μA cm^{-2}. Stanford *et al.*[42] explored laser-induced graphene (LIG) composites as a promising class of triboelectric materials for TENGs. By applying infrared laser irradiation, the surfaces of two carbon-based materials, polyimide (PI) and cork, were transformed into LIG. Using a LIG/PI composite, they fabricated TENGs with both conductor-to-dielectric and metal-free dielectric-to-dielectric configurations, achieving open-circuit voltages exceeding 3.5 kV and peak power outputs greater than 8 mW. Parandeh *et al.*[43] fabricated a flexible TENG utilizing a silk fibroin (SF) fibrous layer combined with a polycaprolactone/graphene oxide composite. Their results demonstrated that surface modification with GO nanosheets greatly enhanced the device's performance. The optimized GO-modified layer achieved a voltage output of 100 V, a current of 3.15 mA, and a power density of 72 mW. Recently, Hatta *et al.*[44] introduced a composite TENG consisting of a PDMS polymer matrix, barium titanate nanopowders as dielectric fillers, and graphene quantum dots as conductive elements. The device demonstrated enhanced performance, with an open-circuit voltage of approximately 310 V, a short-circuit current of 23 μA, and a power density of 1.6 W m^{-2}. However, despite these efforts, the TENGs either involved a complex manufacturing process or used multi-component materials, which ultimately made their production more challenging. Compared to these devices, we developed a high-output TENG using a simple and versatile electrospinning technique with commercially available PVDF-HFP and graphene fillers. This offers the advantages of high performance and low cost, making it an efficient device for energy harvesting.

Finally, it is important to note that the dispersion quality and homogeneity of graphene within the PVDF-HFP matrix are essential for optimizing charge transfer and dielectric properties in TENGs. Graphene aggregation can lead to uneven charge distribution, a reduced effective surface area, and potentially hinder overall device performance. Further examination of dispersion techniques would be valuable, with approaches such as ultrasonication, surface functionalization of graphene, or the use of surfactants to enhance graphene distribution within the PVDF-HFP matrix. Characterization methods such as transmission electron microscopy (TEM) or Raman mapping could offer insights into the dispersion quality and its impact on TENG performance. These will be the focus of our future studies.

4. Conclusions

We have successfully engineered a high-performance TENG by incorporating graphene nanofillers into PVDF-HFP *via* electrospinning to create a nanofibrous mat. Our 15 wt% graphene/PVDF-HFP electrospun nanofiber TENG achieved a peak output voltage of 1024 V and a current density of 1.11 μA cm^{-2}. The impressive electrical performance of this system is attributed to its high dielectric constant and significant charge transfer, which enhance its ability to capture and store triboelectric electrons. Additionally, the TENG demonstrated a maximum output power density of 1.95 W m^{-2} at 50 MΩ and maintained stable performance over extended periods, showing no degradation after 2 weeks. The graphene-based TENGs may offer a sustainable power solution for small devices and have the potential to serve as large-scale generators for harvesting energy in the future.

Data availability

The data supporting this article have been included in the article.

Author contributions

Conceptualization: conceptualization: C.-H. Lee and M.-F. Lin; funding acquisition S.-J. Liu.; investigation: C.-H. Lee, W.-K. Huang, and Y.-H. Kuo; data curing: W.-K. Huang and H. Ito; resources: M.-F. Lin and H. Ito; writing: S.-J. Liu; supervision S.-J. Liu.

Conflicts of interest

The authors declare no conflict of interest regarding the publication of this paper.

Acknowledgements

Financial support was provided by the National Science and Technology Council, Taiwan (Contract No. 111-2221-E-182-004-MY3) and the Chang Gung Memorial Hospital (Contract No. CMRPD2P0071).

References

1 R. Walden, C. Kumar, D. M. Mulvihill and S. C. Pillai, Opportunities and challenges in triboelectric nanogenerator (TENG) based sustainable energy generation technologies: a mini-review, *Chem. Eng. J. Adv.*, 2022, **9**, 100237.

2 J. Zhu, M. Zhu, Q. Shi, F. Wen, L. Liu, B. Dong, A. Haroun, Y. Yang, P. Vachon, X. Guo, T. He and C. Lee, Progress in TENG technology—A journey from energy harvesting to nanoenergy and nanosystem, *EcoMat*, 2020, **2**(4), e12058.

3 G. Zhu, B. Peng, J. Chen, Q. Jing and Z. L. Wang, Triboelectric nanogenerators as a new energy technology: from fundamentals, devices, to applications, *Nano Energy*, 2015, **14**, 126–138.

4 S. Pan and Z. Zhang, Fundamental theories and basic principles of triboelectric effect: a review, *Friction*, 2019, **7**, 2–17.

5 X. Chen, Z. Ren, M. Han, J. Wan and H. Zhang, Hybrid energy cells based on triboelectric nanogenerator: from principle to system, *Nano Energy*, 2020, **75**, 104980.

6 A. Arrigoni, L. Brambilla, C. Bertarelli, G. Serra, M. Tommasini and C. P. Castiglioni, (VDF-TrFE) nanofibers: structure of the ferroelectric and paraelectric phases through IR and Raman spectroscopies, *RSC Adv.*, 2020, **10**, 37779.

7 Y. W. Kim, H. B. Lee, J. Yoon and S. H. Park, 3D customized triboelectric nanogenerator with high performance achieved *via* charge-trapping effect and strain-mismatching friction, *Nano Energy*, 2022, **95**, 107051.

8 M. Sahoo, S. N. Lai, J. M. Wu, M. C. Wu and C. S. Lai, Flexible layered-graphene charge modulation for highly stable triboelectric nanogenerator, *Nanomaterials*, 2021, **11**, 2276.

9 I. Chakraborty, S. N. Lai, M. C. Wu, H. Y. Lin, C. Li, J. M. Wu and C. S. Lai, Charge trapping with a-Fe_2O_3 nanoparticles accompanied by human hair towards an enriched triboelectric series and a sustainable circular bioeconomy, *Mater. Horiz.*, 2021, **8**, 3149.

10 M. Venkatesan, W. C. Chen, C. J. Cho, L. Veeramuthu, L. G. Chen, K. Y. Li, M. L. Tsai, Y. C. Lai, W. Y. Lee, W. C. Chen and C. C. Kuo, Enhanced piezoelectric and photocatalytic performance of flexible energy harvester based on CsZn0.75Pb0.25I3/CNC–PVDF composite nanofibers, *Chem. Eng. J.*, 2022, **433**, 133620.

11 L. Veeramuthu, C. J. Cho, M. Venkatesan, R. Kumar, H. Y. Hsu, B. X. Zhuo, L. J. Kau, M. A. Chung, W. Y. Lee and C. C. Kuo, Muscle fibers inspired electrospun nanostructures reinforced conductive fibers for smart wearable optoelectronics and energy generators, *Nano Energy*, 2022, **101**, 107592.

12 D. W. Kin, J. H. Lee, J. K. Kim and U. Jeong, Material aspects of triboelectric energy generation and sensors, *NPG Asia Mater.*, 2020, **12**, 6.

13 A. Bindhu, A. P. Arun and M. Pathak, Review on Polyvinylidene Fluoride-Based Triboelectric Nanogenerators for Applications in Health Monitoring and Energy Harvesting, *ACS Appl. Electron. Mater.*, 2024, **6**(1), 47–72.

14 V. B. Mbayachi, E. Ndayiragije, T. Sammani, S. Taj, E. R. Mbuta and A. Khan, Graphene synthesis, characterization and its applications: a review, *Results Chem.*, 2021, **3**, 100163.

15 A. R. Urade, I. Lahiri and K. S. Suresh, Graphene properties, synthesis and applications: a review, *JOM*, 2023, **75**, 614–630.

16 F. F. Hatta, M. A. S. M. Haniff and M. A. Mohamed, A review on applications of graphene in triboelectric nanogenerators, *Int. J. Energy Res.*, 2021, **46**, 1–33.

17 R. Zhang and H. Olin, Material choices for triboelectric nanogenerators: a critical review, *EcoMat*, 2020, **2**, e12062.

18 M. Seol, S. Kim, Y. Cho, K.-E. Byun, H. Kim, J. Kim, S. K. Kim, S.-W. Kim, H.-J. Shin and S. Park, Triboelectric series of 2D layered materials, *Adv. Mater.*, 2018, **30**, 1801210.

19 M. Kanik, M. G. Say, B. Daglar, A. F. Yavuz, M. H. Dolas, M. M. El-Ashry and M. Bayindir, A motion- and sound-activated, 3D-printed, chalcogenide-based triboelectric nanogenerator, *Adv. Mater.*, 2015, **27**, 2367–2376.

20 Y. Yang, H. Zhang, J. Chen, Q. Jing, Y. S. Zhou, X. Wen and Z. L. Wang, Single electrode-based sliding triboelectric nanogenerator for self-powered displacement vector sensor system, *ACS Nano*, 2013, **203**(7), 7342–7351.

21 S. Lee, W. Ko, Y. Oh, J. Lee, G. Baek, Y. Lee, J. Sohn, S. Cha, J. Kim, J. Park and J. Hong, Triboelectric energy harvester based on wearable textile platforms employing various surface morphologies, *Nano Energy*, 2015, **12**, 410–418.

22 D. W. Kim, J. H. Lee, I. You, J. K. Kim and U. Jeong, Adding a stretchable deep-trap interlayer for high-performance stretchable triboelectric nanogenerators, *Nano Energy*, 2018, **50**, 192–200.

23 J. P. Lee, B. U. Ye, K. N. Kim, J. W. Lee, W. J. Choi and J. M. Baik, 3D printed noise cancelling triboelectric nanogenerator, *Nano Energy*, 2017, **38**, 377–384.

24 C. Han, C. Zhang, W. Tang, X. Li and Z. L. Wang, High power triboelectric nanogenerator based on printed circuit board (PCB) technology, *Nano Res.*, 2015, **8**, 722–730.
25 T. Huang, M. Lu, H. Yu, Q. Zhang, H. Wang and M. Zhu, Enhanced power output of a triboelectric nanogenerator composed of electrospun nanofiber mats doped with graphene oxide, *Sci. Rep.*, 2015, **5**, 13942.
26 X. X. Wu, J. J. Zhang, C. H. Lee and M. F. Lin, Enhanced triboelectric properties of Eu_2O_3-doped $BaTiO_3$/PVDF-HFP nanofibers, *Nanoscale*, 2023, **15**, 3823.
27 J. Xue, T. Wu, Y. Dai and Y. Xia, Electrospinning and electrospun nanofibers: methods, materials, and applications, *Chem. Rev.*, 2019, **119**(8), 5298–5415.
28 D. Ji, Y. Lin, X. Guo, B. Ramasubramanian, R. Wang, N. Radacsi, R. Jose, X. Qin and S. Ramakrishna, Electrospinning of nanofibres, *Nat. Rev. Methods Primers*, 2024, **4**, 1.
29 L. Shi, H. Jin, S. Dong, S. Huang, H. Huang, H. Xu, J. Chen, W. Xuan, S. Zhang, S. Li, X. Wang and J. Luo, High-performance triboelectric nanogenerator based on electrospun PVDF-graphene nanosheet composite nanofibers for energy harvesting, *Nano Energy*, 2021, **80**, 105599.
30 X. Wang, C. Xiao, H. Liu, Q. Huang and H. Fu, Fabrication and properties of PVDF and PVDF-HFP microfiltration membranes, *J. Appl. Polym. Sci.*, 2018, **135**(40), 46711.
31 S. J. Shen, P. C. Feng, R. C. Wu, Y. H. Kuo and S. J. Liu, Resorbable nanofibrous membranes for local and sustained co-delivery of acyclovir and ketorolac in herpes therapy, *Int. J. Pharm.*, 2024, **654**, 123988.
32 J. H. Zhang, Y. Li, J. Du, X. Hao and H. Huang, A high-power wearable triboelectric nanogenerator prepared from self-assembled electrospun poly(vinylidene fluoride) fibers with a heart-like structure, *J. Mater. Chem. A*, 2019, **7**, 11724–11733.
33 *Broadband Dielectric Spectroscopy*, ed. Kremer F. and Schönhals A., Springer-Verlag, Berlin, Heidelberg, 2003.
34 E. Barsoukov and J. R. Macdonald, *Impedance Spectroscopy: Theory, Experiment, and Applications*, Wiley-Interscience, Hoboken, NJ, 2005.
35 S. A. Shankaregowda, C. B. Nanjegowda, X. Cheng, M. Shi, Z. Liu and H. Zhang, A flexible and transparent graphene based triboelectric nanogenerator, *Proc 15th IEEE Conf Nanotech*, 2015.
36 I. Shabbir, D. M. Lee, D. C. Choo, Y. H. Lee, K. K. Park, K. H. Yoo, S. W. Kim and T. W. Kim, A graphene nanoplatelets-based high-performance, durable triboelectric nanogenerator for harvesting the energy of human motion, *Energy Rep.*, 2022, **8**, 1026–1033.
37 A. A. Pillai, J. John, R. M. Mathew, J. Jose, E. S. Zacharia, R. Abraham, N. M. Johnson, R. L. Thomas and V. Thomas, Enhanced output performance of graphene oxide based triboelectric nanogenerators *via* plasmon coupling, *J. Mater. Sci. Eng. B*, 2023, **296**, 116637.
38 E. J. Jelmy, D. Jose, K. V. Vijoy, K. J. Saji and H. John, Enhanced triboelectric performance of graphene oxide-conducting polymer hybrid modified polydimethylsiloxane composites, *Mater. Adv.*, 2022, **3**, 6897–6907.
39 M. Sahoo, S. N. Lai, J. M. Wu, M. C. Wu and C. S. Lai, Flexible layered-graphene charge modulation for highly stable triboelectric nanogenerator, *Nanomaterials*, 2021, **11**, 2276.
40 I. Domingos, A. I. S. Nerves, M. F. Craciun and H. Alves, Graphene based triboelectric nanogenerators using water based solution process, *Front. Phys.*, 2021, **9**, 742563.
41 F. Ejehi, R. Mohammadpour, E. Asadian, P. Sasanour, S. Fardindoost and O. Akhavan, Graphene oxide papers in nanogenerators for self-powered humidity sensing by finger tapping, *Sci. Rep.*, 2020, **10**, 7312.
42 M. G. Standord, J. T. Li, Y. Chyan, Z. Wang, W. Wang and J. M. Tour, Laser-induced graphene triboelectric nanogenerators, *ACS Nano*, 2019, **13**, 7166–7174.
43 S. Parandeh, M. Kharaziha, F. Karimzadeh and F. Hosseinabadi, Triboelectric nanogenerators based on graphene oxide coated nanocomposite fibers for biomedical applications, *Nanotechnology*, 2020, **31**, 385402.
44 F. F. Hatta, M. A. S. M. Haniff and M. A. Mohamed, Enhanced-performance triboelectric nanogenerator based on polydimethylsiloxane/barium titanate/graphene quantum dot nanocomposites for energy harvesting, *ACS Omega*, 2024, **9**, 5608–5615.